Maritime Engineering
Volume 166 Issue MA2
Using a sand–mud model to hindcast the morphology near Waarde, the Netherlands
Dam and Bliek

ice | proceedings

Proceedings of the Institution of Civil Engineers
Maritime Engineering 166 June 2013 Issue MA2
Pages 63–75 http://dx.doi.org/10.1680/maen.2011.43
Paper 201143
Received 04/12/2011 Accepted 05/03/2013
Keywords: coastal engineering/hydraulics & hydrodynamics/mathematical modelling

ice Institution of Civil Engineers
publishing

Using a sand–mud model to hindcast the morphology near Waarde, the Netherlands

Gerard Dam MSc
Svašek Hydraulics, Rotterdam, and UNESCO-IHE, Delft, the Netherlands

Abraham J. Bliek MSc
Svašek Hydraulics, Rotterdam, the Netherlands

Due to the construction of two cross-shore groynes near Waarde in the Western Scheldt estuary, the Netherlands, morphological changes in the area have occurred. A mud flat has developed between the groynes and at the tip of the groynes scour has occurred which has contributed to channel migration. Both the sand and mud fraction have contributed to this change. In this paper a process-based morphological model is presented that can reproduce most morphological changes thanks to the fact that both fractions are taken into account, as well as the interaction between sand and mud. Using the model, 5 years of morphological changes were simulated from the construction of the groynes onwards. The Brier-skill score of the erosion/sedimentation pattern is 0·35, which means that the model has significant skill and can be classified as reasonable. A regression coefficient of 0·66 is found for the observed and modelled mud content in the bed after 5 years, which means that the model can reproduce the mud content reasonably well for most locations. The model can clearly distinguish between a sand- or mud-dominated area.

Notation

B	initial bed level (m)
c_e	equilibrium sand concentration in the water column (kg/m^3)
c_m	mud concentration in the water column (kg/m^3)
$c_{m,boun}$	mud concentration at boundary (kg/m^3)
c_s	sand concentration in the water column (kg/m^3)
dz	thickness of layer in bed module (m)
F_m	vertical flux of mud (kg/m^2/s)
F_s	vertical flux of sand (kg/m^2 pers)
H	Heaviside function; 0 if argument < 0; 1 if argument $\geqslant 0$
M_c	erosion coefficient of cohesive bed (kg/m^2 per s)
M_{nc}	erosion coefficient of non-cohesive bed (kg/m^2 per s)
MF	morphological acceleration factor
n	number of layers in bed module
p_m	mud content of the top bed layer
$p_{m,cr}$	critical mud content for cohesive behaviour
$p_{m,init}$	initial mud content for cohesive behaviour
$p_{m,sub}$	mud content in sub-layer
w_m	fall velocity of mud (m/s)
w_s	fall velocity of sand (m/s)
X	computed bed level (m)
Y	measured bed level (m)
z_b	vertical coordinate of bed surface (m)
z_c	distance below the bed surface z_b (positive downwards) (m)
Θ	mixing coefficient (m^2/s)
ρ_{silt}	density of silt (kg/m^3)
τ_b	bottom shear stress due to current and waves (Pa)
τ_d	critical shear stress for deposition of mud (Pa)
$\tau_{e,c}$	critical bottom shear stress for cohesive bed (Pa)
$\tau_{e,nc}$	critical bottom shear stress for non-cohesive bed (Pa)

1. Introduction

In 2002 two cross-shore groynes were constructed at an intertidal area near Waarde in the Western Scheldt estuary in the south-west of the Netherlands (Figure 1). These groynes are designed to protect the intertidal area from eroding. By building the groynes the tidal velocities have reduced, resulting in accretion of sediment between the groynes. The composition of this sediment is a sand–mud mixture, whereas the bed material directly in front of the groynes is mainly sand. The construction of the groynes also affected the migration of channels in the direct vicinity. This suggests that in the area there is a lot of interaction between the sand and the mud regime.

This paper presents the setting up of a process-based morphological model, which includes both the sand and mud

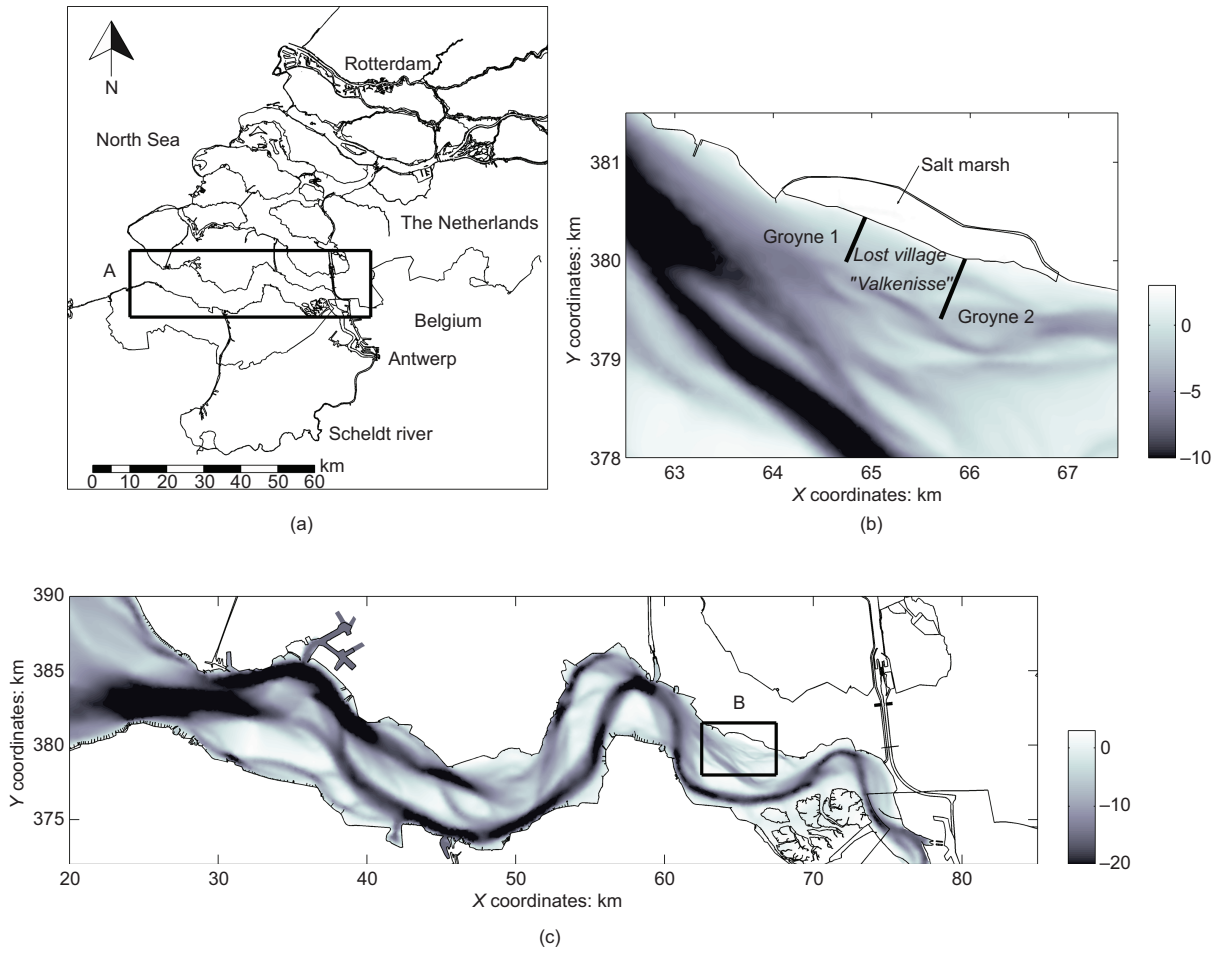

Figure 1. Western Scheldt and study area; depths of 2002: (a) general overview; (b) area of interest; (c) Western Sheldt estuary. Depths in m MSL

fraction and their interaction in order to hindcast the morphological changes in the area. This model differs from a classical morphological model which would describe the sand and mud fractions separately, rather than both fractions at the same time, and would be unable to represent the interaction between the fractions. A calibration on the field observations from 2002 to 2007 was carried out.

The model is a finite-element-based model called FINEL2d using an unstructured grid with triangular elements to describe the complete Western Scheldt estuary. For the purpose of this study the grid was strongly refined in the area of interest. Around the groynes a grid size of about 10 m was applied to have sufficient resolution for the flow pattern near the groynes.

The content of this paper is as follows: in Section 2 a description of the study area is given. The set-up of the FINEL2d model of the Western Scheldt is discussed in Section 3. Section 4 describes the model results. Finally in Section 5 the conclusions of this study are given.

2. Description of study area

The Western Scheldt estuary is a dynamic multiple channel system that has gone through many changes due to human impacts and natural developments. The morphology of the Western Scheldt is very important for all functions related to this area, such as navigation, ecology and sand mining.

The estuary is approximately 70 km long and 4 km wide. The tidal range increases from 3·9 m at the mouth to 5·0 m near Antwerp (Figure 1). One of the main channels is the navigational channel to the port of Antwerp. Maintenance dredging takes place to keep the navigational channel at the required depth. The Western Scheldt consists mainly of fine

non-cohesive sediments. Mud is mainly found on intertidal areas. These intertidal areas are valuable for the ecology. The intertidal area consists of sand banks, mudflats and salt marshes.

The morphological changes in the Western Scheldt are dominated by the tidal motion. The river discharge is of minor importance as the freshwater discharge is only 0·6% of the tidal prism at the mouth (Van der Spek, 1997). The Western Scheldt estuary is a well-mixed estuary.

In the past centuries storm surges have caused major flooding. Many villages were flooded and lost to the sea. The intertidal area near Waarde (at the area of interest) showed an eroding trend causing the remains of one of these villages called 'Valkenisse' to become exposed at the sea bed surface. To stop the trend of erosion and to protect the remains, two groynes were constructed in 2002 (Figure 1). The length of the groynes is approximately 500 m. The height of the groynes is around mean high water spring at the landward side (+2·5 m mean sea level (MSL) and around MSL at the seaward end). After construction of the groynes a transition occurred from a trend of erosion to sedimentation and from sand-domination to mud-domination in the area between and around the groynes.

The area of interest is sheltered against waves, although the dominant wind direction in the Netherlands is south-west. The intertidal area in front of the groynes makes the wind fetch length and thus the waves relatively small. A survey campaign in 1996 showed an average significant wave height of 0·2 m on the intertidal area (Koster Engineering, 1997). As the Western Scheldt estuary is relatively shallow with a sheltered position, the impact of tides exceeds the wave action by far (Van der Spek, 1997), although they most likely contribute to some intertidal morphodynamic behaviour. The dominant forcing is the tidal flow, carrying both sand and mud. The long-term average mud concentration in the water is approximately 60 mg/l in the area of interest (Rijkswaterstaat, 2012). During a neap–spring cycle and over the seasons the concentration in the Western Scheldt varies by a factor of 1·5–2 (Van der Wal *et al.*, 2010). Storms can cause large peaks in the concentration.

Figure 2(a) shows the bed level in 2002, prior to the construction of the groynes. Figure 2(b) shows the bed level in 2007, 5 years after construction. The difference between Figure 2(a) and (b) can be seen in Figure 6(a) later. A number of morphological changes have occurred in the area, partly due to the presence of the groynes and partly due to estuary-wide behaviour of the area. Locations a, b and c in Figure 2 show sedimentation caused by the groynes. The sedimentation has become over 1 m here over the 5-year period and consists mainly of mud. At the tip of the eastern groyne a large scour hole can be seen (d), while the eastern groyne shows less scour (e). The Zimmerman channel, a sand-dominated channel located just east of the groyne area, shows a decrease in depth and a migration to the north (g). The channel is split into a flood (h) and ebb channel (f) that ends near the eastern groyne. In the Schaar van Waarde channel, which is a flood-dominated channel located south-west of the area of interest, some changes have also occurred. Locations j and k in Figure 2 show erosion, whereas the small channel (i) shows sedimentation. Location I at the south side of the Schaar van Waarde channel shows a build-up of sediment along the border of the channel. The locations d to l are in the sand-dominated area with only a few per cent of mud in the bed (McClaren, 1994).

3. Description of the sand–mud model

3.1 Introduction

Process-based morphological models have developed rapidly during recent decades. The models are becoming increasingly robust tools for predicting morphodynamic developments based on physical descriptions and advanced bed update techniques (Van der Wegen and Roelvink, 2012). The focus of most model applications with dynamic bed development is on non-cohesive sediments (sand). Hibma *et al.* (2003, 2004), Marciano *et al.* (2005), Van der Wegen and Roelvink (2008, 2012) and Van der Wegen *et al.* (2008) have shown that it is possible to use process-based models to reproduce channel-shoal formation in a tidal inlet or estuary starting in an idealised way from an initially flat bed.

Classically separate models are used for sand (Van Rijn, 1993) and mud (Van Kessel *et al.*, 2010; Winterwerp and Van Kesteren, 2004). Sand models have a dynamic coupling between bed level changes and the water motion, whereas mud models generally do not have this coupling (Van Ledden, 2003). The focus of this research is on hindcasting the bed dynamics in an area where both cohesive and non-cohesive sediments are present. This requires not only the integration of 'sand' and 'mud' (non-cohesive and cohesive) processes in one model but also the interaction between sand and mud.

3.2 Set-up of the sand–mud model

Following Van Ledden *et al.* (2004a, 2004b), in the present study a sand–mud model was used in which both sand and mud and their interaction contributed to morphological changes. Earlier research with a sand–mud model has been carried out by Van Ledden (2003), Van Ledden *et al.* (2004b), Dam *et al.* (2005), and Paarlberg *et al.* (2005). The set-up of this model is shown in Figure 3. There are a few reasons why this approach has advantages over a classical approach in which sand and mud are treated separately. The first reason is that both sand and mud contribute to morphological change (arrows 3 and 4 in Figure 3) and both fractions have a dynamic coupling with the water motion (arrow 8). The second reason is

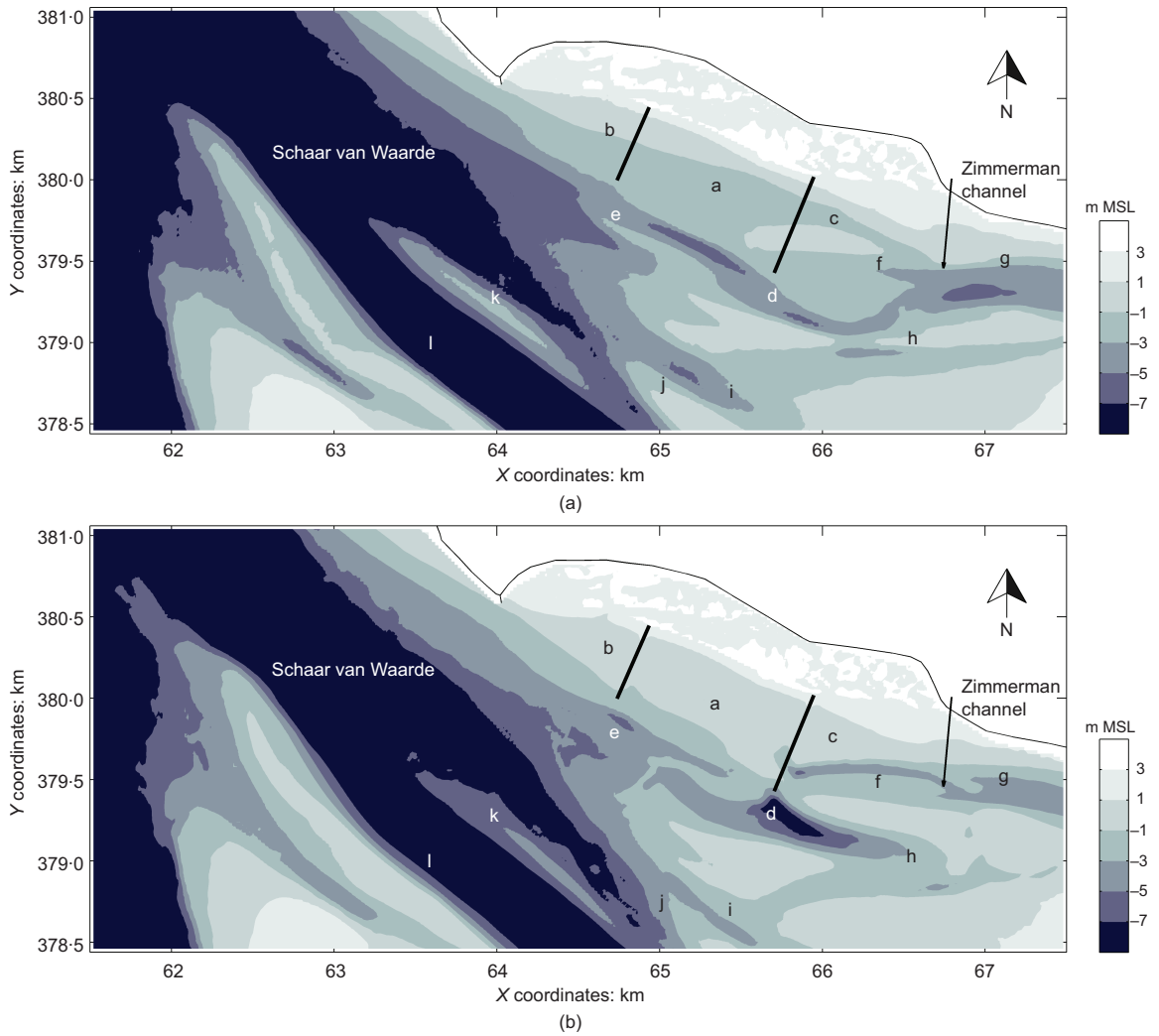

Figure 2. Observed bed levels in (a) 2002 and (b) 2007 in the study area

that the erosion of sediment is limited by the availability of sand or mud in the bed due to the bed module (arrows 6 and 7). The third reason is that the interaction between sand and mud in the bed is taken into account (also arrows 6 and 7). Non-cohesive behaviour of the bed occurs when the mud content in the bed is below a critical mud content value. Cohesive behaviour of the bed occurs when the mud content is above this value. Cohesive behaviour will harden the bed, making it more difficult to erode. This is described through the erosion coefficient and critical shear stress for erosion. Both the non-cohesive state and cohesive state are described in detail below.

3.2.1 Non-cohesive state of the bed

When the mud content in the bed (p_m) is below the critical mud content ($p_{m,cr}$) the bed layer is treated as non-cohesive. This implies for the sand fraction that the normal sediment transport formula is used, in this case the Engelund–Hansen formula (Engelund and Hansen, 1967). The Engelund–Hansen formula is used to calculate an equilibrium concentration c_e. If the sand concentration in that grid point is below the equilibrium concentration, erosion occurs; if it is above, sedimentation. In this way the vertical flux of sand is described – see Equation 1 in Table 1. However, in the case of erosion of sand from the bed, the vertical flux is limited by the availability of sand in the bed which is described by the term $(1 - p_m)$.

Following Van Ledden *et al.* (2004b), the vertical flux of mud is described by Equation 2 in Table 1, in which the first part describes the erosion flux (cf. Partheniadis, 1965) and the second part the deposition flux (cf. Krone, 1962).

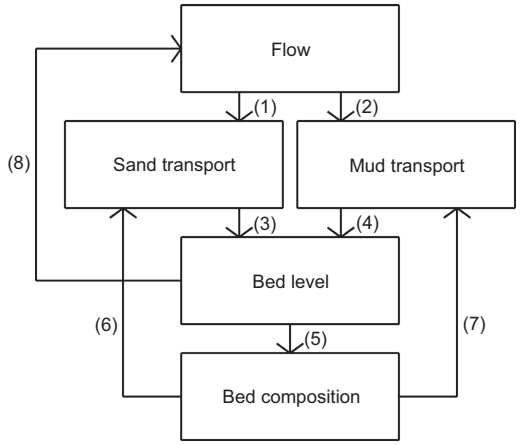

Figure 3. Set-up of the sand–mud model (after Van Ledden, 2003)

3·2.2 Cohesive state of the bed

Cohesive sand–mud mixtures have shown that the erosion characteristics strongly differ from non-cohesive sand–mud mixtures (Mitchener and Torfs, 1996). Therefore erosion of a cohesive bed is treated differently in the model by using a separate erosion coefficient and critical shear stress for a cohesive bed. The key element is that the erosion formula for sand and mud is equal, assuming a sand–mud mixture; however, the flux is further dependent on the availability of sand or mud in the bed module. This is expressed in the first part of Equations 3 and 4 in Table 2 which denotes the erosion part (Van Ledden *et al.*, 2004b). The second part of Equations 3 and 4 describes the deposition part and is equal to the non-cohesive state (Equation 1 and 2 in Table 1).

3.2.3 Bed module

A bed module consisting of several layers of the sea bed was used to account for the sand–mud content of the bed. In Figure 4 the bed module is given schematically. A number of layers (n) are defined below the sea bed with thickness dz.

Using a Lagrangian coordinate system the layers move up and down following the bed level changes while maintaining a fixed thickness dz. The bed composition of the layers varies in time and space, induced by upward and downward fluxes of sand and mud at the bed surface, and by physical and biological mixing in the sediment layers below. The mud content in the bed is thus described by Equation 5. A mixing coefficient is introduced to account for the physical and biological mixing. Physical mixing occurs when the bed is stirred by flow and/or waves. Biological mixing consists of organisms that move through the bed and mix the sediments (Van Ledden, 2003).

$$5. \quad \frac{\partial p_m}{\partial t} + \frac{\partial z_b}{\partial t}\frac{\partial p_m}{\partial z_c} - \frac{\partial}{\partial z_c}\left(\Theta \frac{\partial p_m}{\partial z_c}\right) = 0$$

where z_b is the vertical coordinate of the bed surface (m), Θ is the mixing coefficient (m^2/s), and z_c is the distance below the bed surface z_b (positive downwards) (m).

In the sub-layer a fixed mud percentage ($p_{m,sub}$) must be applied. This mud percentage becomes important in an eroding case. In that case this sub-layer mud percentage is introduced in the lowest layers. For more information of the bed module and the numerical implementation of the bed module refer to Van Ledden (2003).

3.3 Description of the Western Scheldt model

The process-based model that was applied in this study is called FINEL2d. The model is a two-dimensional horizontal (2DH) process-based model based on the finite-element method. The depth-integrated shallow water equations are the governing equations of the flow module. For details about FINEL2d refer to Dam *et al.* (2007).

Equation	Fraction	Non-cohesive state of bed ($p_m \geqslant p_{m,cr}$)
(1)	Sand	$F_s = (1-p_m)w_s c_e - w_s c_s$
(2)	Mud	$F_m = p_m M_{nc}\left(\frac{\tau_b}{\tau_{e,nc}} - 1\right) H\left(\frac{\tau_b}{\tau_{e,nc}} - 1\right) - w_m c_m \left(1 - \frac{\tau_b}{\tau_d}\right) H\left(1 - \frac{\tau_b}{\tau_d}\right)$

F_s, vertical flux of sand (kg/m^2 per s); F_m, vertical flux of mud (kg/m^2/s); w_s, fall velocity of sand (m/s); w_m, fall velocity of mud (m/s); c_s, sand concentration in the water column (kg/m^3); c_e, equilibrium sand concentration in the water column (kg/m^3); c_m, mud concentration in the water column (kg/m^3); p_m, mud content of the top bed layer; $p_{m,cr}$, critical mud content for cohesive behaviour; M_{nc}, erosion coefficient of non-cohesive bed (kg/m^2 per s); τ_b, bottom shear stress due to current and waves (Pa); τ_d, critical shear stress for deposition of mud (Pa); $\tau_{e,nc}$, critical bottom shear stress for non-cohesive bed (Pa); H, Heaviside function – equals 0 if argument < 0; equals 1 if argument $\geqslant 0$.

Table 1. Vertical flux formulas for sediment exchange between water and bed (non-cohesive state)

Equation	Fraction	Cohesive state of bed ($p_m > p_{m,cr}$)
(3)	Sand	$F_s = (1-p_m)M_c\left(\frac{\tau_b}{\tau_{e,c}}-1\right)H\left(\frac{\tau_b}{\tau_{e,c}}\right)-w_s c_s$
(4)	Mud	$F_m = p_m M_c\left(\frac{\tau_b}{\tau_{e,c}}-1\right)H\left(\frac{\tau_b}{\tau_{e,c}}-1\right)-w_m c_m\left(1-\frac{\tau_b}{\tau_d}\right)H\left(1-\frac{\tau_b}{\tau_d}\right)$

M_c, erosion coefficient of cohesive bed (kg/m^2 per s); $\tau_{e,c}$, critical bottom shear stress for cohesive bed (Pa).

Table 2. Vertical flux formulas for sediment exchange between water and bed (cohesive state)

FINEL2d uses an unstructured triangular grid. The advantage of such a mesh in comparison with, for example, a finite-difference grid is the flexible mesh generation. In FINEL2d no nesting techniques are required in regions of specific interest, where a higher degree of resolution is needed, whereas arbitrary coastlines and complex geometries can be resolved very well.

The basis for the grid is the Western Scheldt model as described in Dam *et al.* (2007). Near the area of interest the grid is refined to a grid size of approximately 10 m, so that the flow pattern over and around the groynes can be computed in detail, as well as the morphological development of small channels. The grid can be seen in Figure 5, zooming in three steps from the overview of the full grid to the mesh details in the groyne area. The groynes are shown as thick black lines in Figure 5(b). The groynes are schematised as weirs on a line element in the grid. In reality, conservation of energy holds upstream of the weir and conservation of momentum downstream. The standard model solves the momentum equations both upstream and downstream of the weir, leading to an inaccurate solution. Weir formulations are therefore required to calculate the correct discharges over the groyne. The implemented empirical weir formulation that is used is based on laboratory results by Sieben (2007). Numerically the implementation is based on Garcia-Navarro and Saviron (1992).

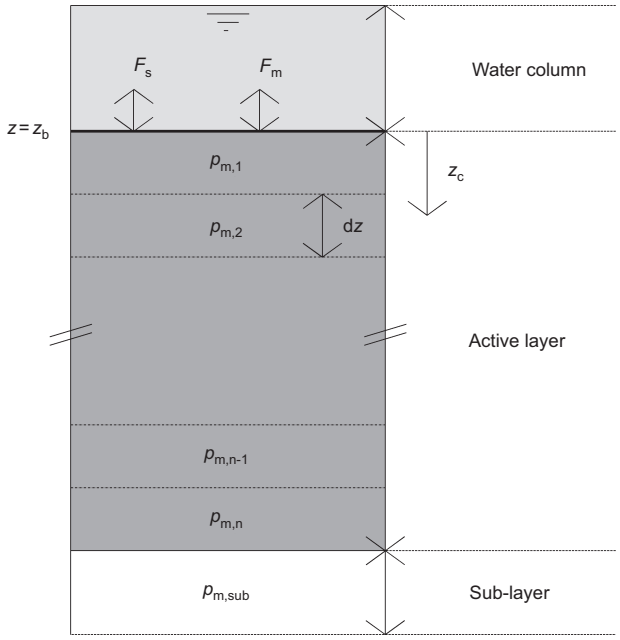

Figure 4. Bed module (after van Ledden, 2003)

On the seaward side of the grid, tidal boundary conditions are given, whereas on the river side, constant (small) river discharges are taken. The effect of freshwater is not included in the model as the river discharge is small and no significant freshwater effects on the water dynamics are present in the area of interest.

3.4 Model calibration

The calibration of the model on the water motion and the sandy morphology for the entire Western Scheldt estuary has already been carried out and is reported in Dam *et al.* (2007). In that calibration the mud fraction was ignored as mud is only important for a relatively small area of intertidal areas. For the main channel morphology the mud behaviour is not very relevant. In the present study the morphological model of the Western Scheldt is extended with the mud fraction. The sand–mud model is calibrated on the area of interest. The calibration process is described in detail here.

Outside a range of 5 km around the area of interest the mud concentration in the model is taken to be constant at 60 mg/l (being the average natural mud concentration in the water). Inside the 5 km range the mud concentration in the water is calculated by the model. The available mud concentration measurements in the area of interest (Rijkswaterstaat, 2012) are limited to taking water samples every few weeks for several years. This gives an estimate of the average concentration, but time series of the mud concentration over a tidal cycle are not available in the area of interest. Hence calibration on the mud

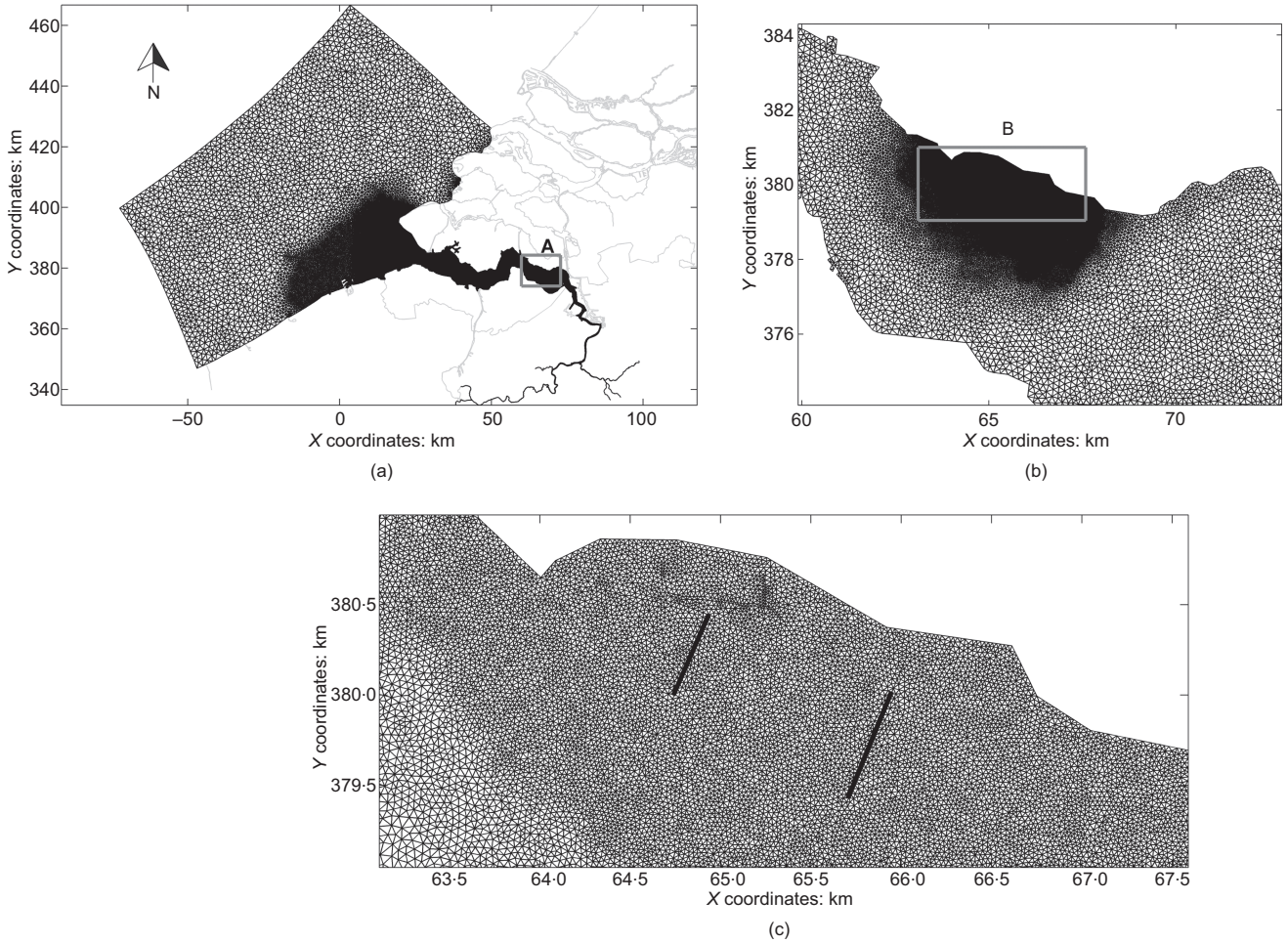

Figure 5. Computational grid of FINEL2d model

concentrations is not possible. It is therefore assumed that since the average concentration of 60 mg/l is applied outside a 5 km range around the area of interest the tidal forcing will transport this average mud concentration in the area near the groynes.

The sand concentration is calculated by the model over a large area around the area of interest without fixed settings.

To speed up the calculation a morphological acceleration factor (*MF*) is used every time-step to multiply the bed level changes (Roelvink, 2006). In this case an *MF* of 24·75 is applied in accordance with Dam *et al.* (2007). One neap–spring cycle for the water motion represents a morphodynamic year with this setting.

In 2002 the mud contents in the top layer were measured at the mudflat (Sistermans *et al.*, 2007). The values were interpolated to the computational grid and used as the initial mud content in the bed. Outside the area of interest the initial mud content in the bed was taken at 2%. This corresponds to the average mud percentage in the sand-dominated regime of the estuary (McClaren, 1994). As the saltmarsh north of the mudflat was not flooded and therefore not morphologically active during the computation, the initial mud content was also chosen at an arbitrary 2%. The resulting initial mud content that was used as input is shown in Figure 7(a) below. The critical mud content for cohesive behaviour of the bed was set at 30%, based on Van Ledden (2003).

It is known that biological activity has influence on cohesive sediment transport on a seasonal scale (Borsje *et al.*, 2008; Winterwerp and Van Kesteren, 2004). In the present study the settings for the cohesive sediment parameters were chosen in such a way that they represent a complete year, neglecting the seasonal variation.

Several calculations were carried out in which the optimal parameter settings were found. Generally, the erosion–sedimentation pattern is not very sensitive for different realistic

parameter settings. The parameter settings merely control the level of changes. The parameter settings which are presented in Table 3 best represent the observed bed level changes. An exception to the low sensitivity is the mixing coefficient Θ which more or less controls the mud content in the top layer. The mixing coefficient is calibrated so that it best represents the observed mud content in 2007. Note that this mixing coefficient hardly affects the bed level. For more information about the calibration of the sand–mud model refer to Dam (2008).

The outcome of the calibration of the area of interest is presented in Section 4.

4. Results

4.1 Introduction

Using the FINEL2d model with the settings as described in Table 3, a time period of 5 years of morphodynamic development was simulated. The starting point is the bathymetry in 2002, just after completion of the groyne construction, as can be seen in Figure 2(a). The model produced bed levels, mud content in the bed, and concentrations. For the comparison between the model results and field data the observed and calculated bathymetry was used. The mud content of the top layer in 2007 was measured at several locations and compared with the model outcomes. Due to lack of field data the predicted suspended sediment concentration was not compared with observations.

4.2 Observed and modelled morphological developments

The observed and calculated erosion and sedimentation pattern can be seen in Figure 6. The locations (a) to (l) in Figure 6 correspond to the same locations in Figure 2. Note that Figure 6(a) presents the observed changes in sea bed level over the years 2002 to 2007. In fact, Figure 6(a) is the differential plot of Figure 2(a) and (b). Figure 6(b) gives the model result on erosion and sedimentation. For comparison reasons, the locations (a) to (l) are also indicated in this Figure. In Figure 7 the mud content of the surface layer of the sea bed as calculated in 2007 is presented together with measured mud content in 2007 at several locations on the mudflat (Escaravage *et al.*, 2007).

The development of the locations (a) to (l) as indicated in the figures is discussed in detail here.

Coefficient	Symbol	Setting
Morphology		
Morphological acceleration	MF	24·75
Non-erodible layers		Data of 2001
Sand fraction		
Formula		Engelund–Hansen (1967)
Grain size	d_{50}	200 μm
Fall velocity of sand	w_s	0·015 cm/s
Mud fraction		
Fall velocity of mud	w_m	0·001 m/s
Critical shear stress for sedimentation	τ_s	0·5 Pa
Mud concentration at boundary	$c_{m,boun}$	60 mg/l
Density	ρ_{silt}	750 kg/m^3
Bed module		
Number of layers	n	5
Layer thickness	dz	0·25 m
Mud content sub-layer	$p_{m,sub}$	0%
Sand–silt interaction		
Critical mud content in bed	$p_{m,cr}$	30%
Critical shear stress for erosion (cohesive bed)	τ_c	0·75 Pa
Critical shear stress for erosion (non-cohesive bed)	τ_{nc}	0·2 Pa
Erosion parameter (cohesive bed)	M_c	0·0001 kg/m^2 per s
Erosion parameter (non-cohesive bed)	M_{nc}	0·001 kg/m^2 per s
Initial mud content in bed	$p_{m,init}$	2%
Mixing coefficient	Θ	0·0000025 m^2/s

Table 3. Optimal model settings

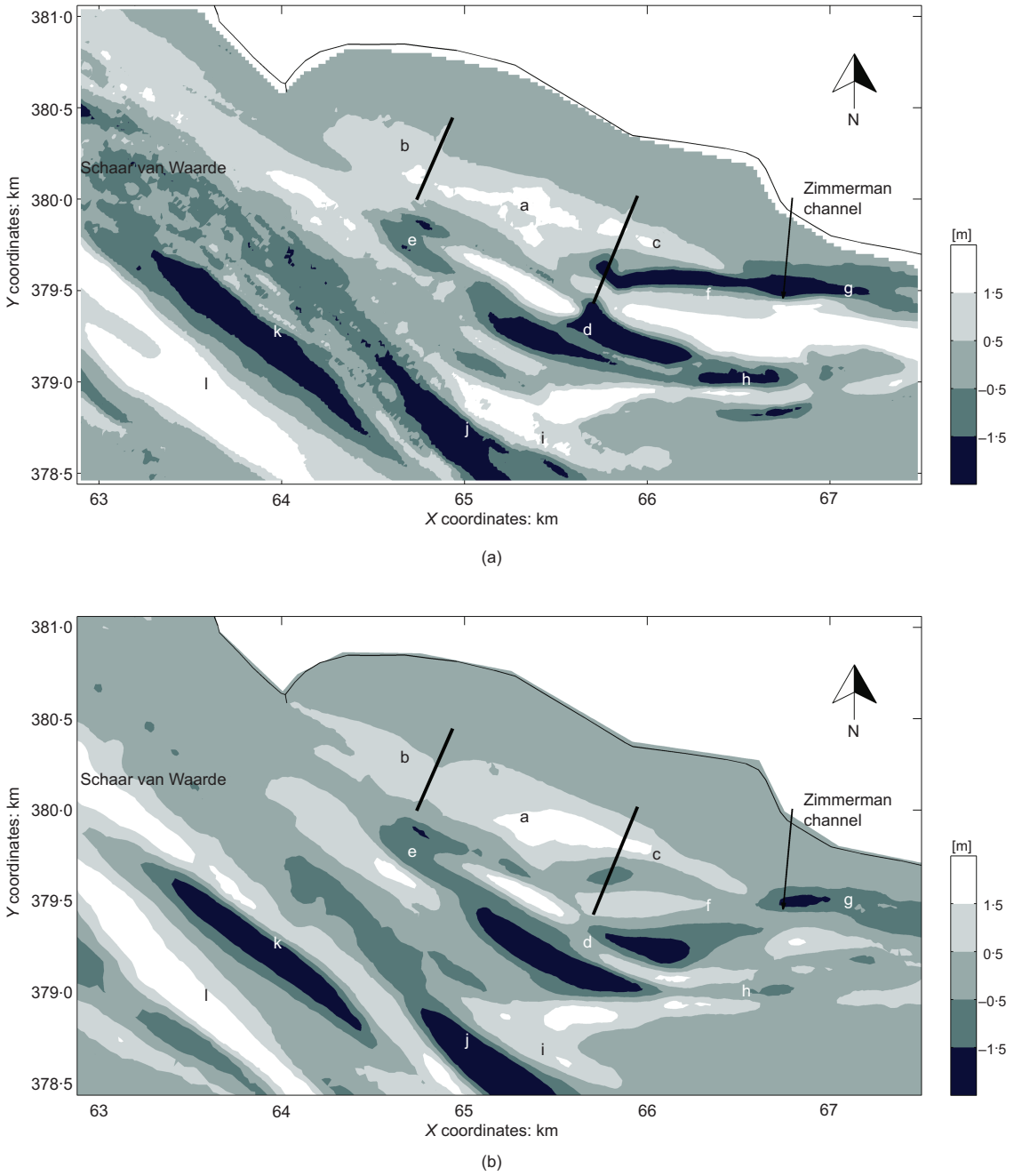

Figure 6. (a) Observed and (b) calculated erosion–sedimentation pattern 2002–2007

The sedimentation in the locations a, b and c is fairly well reproduced by the model when comparing Figure 6(a) and 6(b). The sedimentation in the model at these locations is partly mud (Figure 7). The scour that has occurred around the eastern groyne (location d in Figure 4) was reproduced by the model, albeit with too small a magnitude. At location e a small scour can be seen around the eastern tip of the western groyne in the observations. The model calculates the erosion at the tip of the western groyne in accordance with the observations. The migration of the Zimmerman channel to the north (g) can both be seen in the observations and the model, although the separation of the channel into a flood (h) and ebb channel (f) is

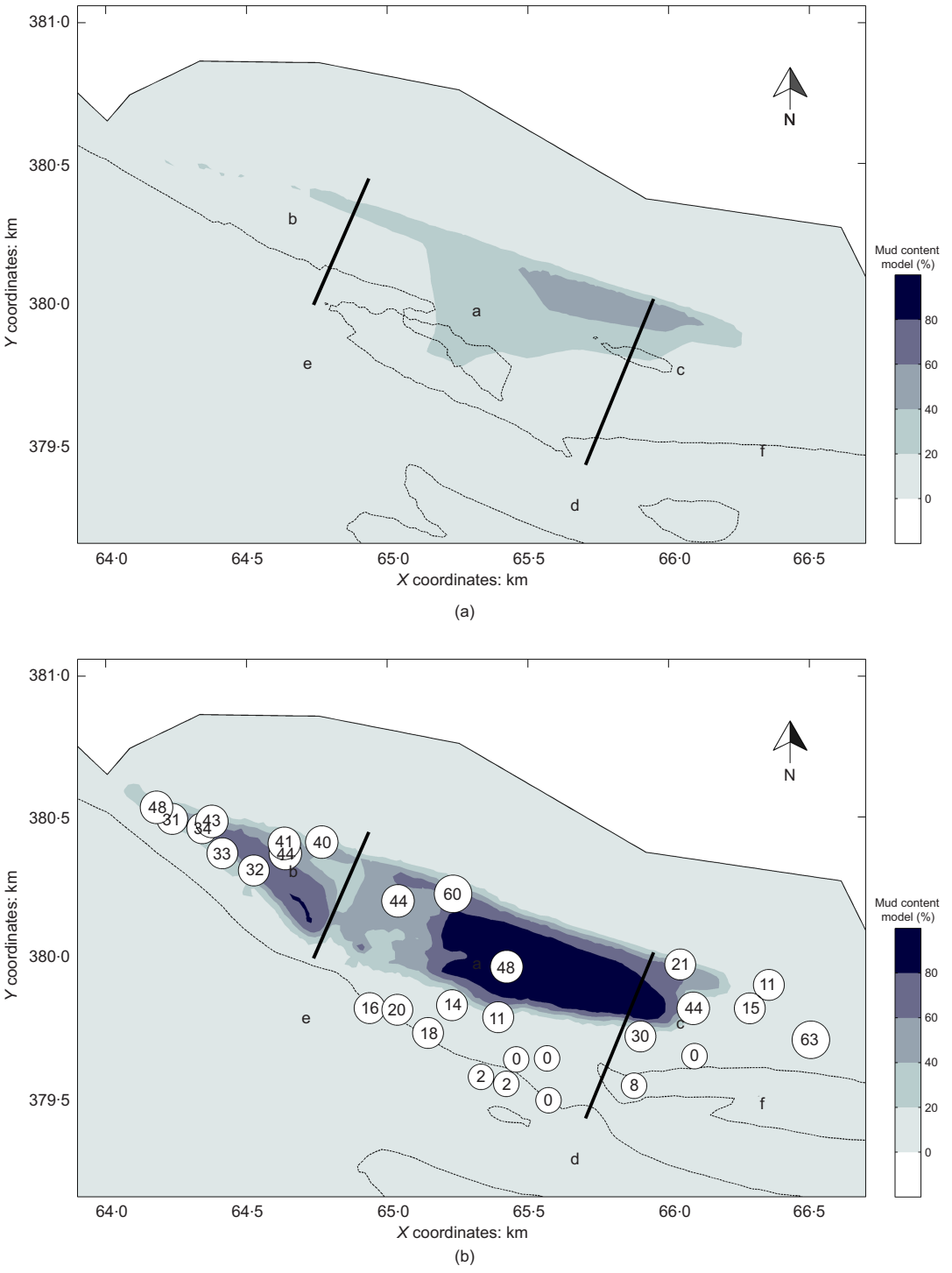

Figure 7. (a) Initial (observed) mud content (%) of the model in 2002 (input) and (b) modelled and observed mud content in 2007 (output). In white circles: measured mud content (%) in 2007 (Escaravage *et al.*, 2007); dashed contour line is −2 m MSL of 2002 and 2007

insufficiently calculated by the model. The erosion of the Schaar van Waarde channel is probably outside the morphological influence of constructions of the groynes. The results here represent the autonomous behaviour of the area, which means that the morphodynamic changes would have been the same if the groynes had not been constructed. The model results are in line with the observations: the erosion in the Schaar van Waarde channel is calculated correctly by the model in location j and k. The filling of the small channels at location i is also calculated by the model. The sedimentation south of the Schaar van Waarde channel at location l is reproduced by the model.

In order to quantify the model results objectively the Brier-skill score (BSS) was used as defined in Equation 6 (Sutherland *et al.*, 2004). The BSS reflects how good the model results are in comparison with the observed change. Note that this index only refers to measured and observed bed changes. It does not take into account the mud content in the sea bed.

$$6. \quad \mathrm{BSS} = 1 - \frac{\langle (Y-X)^2 \rangle}{\langle (B-X)^2 \rangle}$$

where X is the computed bed level (m), Y is the measured bed level (m), B is the initial bed level (m) and $\langle\,\rangle$ denotes the arithmetic mean.

Van Rijn *et al.* (2003) defined the following classification of the BSS

Excellent: 1·0–0·8

Good : 0·8–0·6

Reasonable/fair: 0·6–0·3

Poor: 0·3–0·0

Bad: < 0

A BSS of 1 means a perfect match between measurements and model results, whereas a result below 0 suggests that the model result is worse than zero bed changes. The BSS is calculated using the measured erosion–sedimentation pattern and the modelled erosion–sedimentation pattern as shown in Figure 6. The BSS value using Equation 6 is 0·35, which means that the model has significant skill and produces reasonable results according to Van Rijn *et al.* (2003). Note that this BSS value does not take into account error contributions from survey data, the error in methodology used to refer the measurement to a vertical datum and the error in the methodology used to interpolate measured changes onto the model grid. Taking into account an error contribution would make the BSS value higher.

4.3 Observed and modelled mud content in the bed

The observed and modelled mud content in the top layer of the bed in 2007 is shown in Figure 7(b). The agreement between a cohesive ($> 30\%$ mud) and non-cohesive bed ($<30\%$ mud) can reasonably be reproduced by the model. A high content of mud was present both in the model and in the measurements at the north side of the mudflat close to the tidal marsh. It does not seem possible to model the difference between a high mud content ($> 30\%$ and $< 40\%$) and a very high mud content ($> 40\%$), although the number of observations in the mud-dominated region are too low to really conclude this. At the east side of the area (near c) the modelled mud content is somewhat too low in comparison with the data. An area can be seen between the tips of the groynes in Figure 7 that is clearly sand-dominated in both the model and the measurements (roughly between a, d and e). The rest of the domain outside the direct influence of the groynes is sand-dominated (McClaren, 1994). This is reproduced by the model ($< 20\%$ mud in Figure 7). When the measured and the calculated mud content of the observation points are compared using regression analysis a regression coefficient (R) of 0·66 is obtained, which suggests that the model can reproduce the observed mud content reasonably well. It should be noted that the observations represent the mud content at the time of the measurement. The mud content in the field can be sensitive to seasonal and storm fluctuations, whereas the model does not take these fluctuations into account. It is important to conclude here that an increase of the mud content over the years has occurred around the groynes, that a clear separation of sand and mud in the field can be seen, and that these two phenomena are reproduced by the model.

5. Conclusions

It can be concluded that the morphological development of the tidal flat and the adjacent channel systems in the Schaar van Waarde (Western Scheldt) after construction of two cross-shore groynes are determined by cohesive and non-cohesive sediment transport processes, and by the interaction between these processes.

By applying the sand–mud module of the FINEL2d model, most of the morphological developments in the area can be reasonably reproduced over a period of 5 years after construction of the groynes. The BSS of the erosion–sedimentation pattern is 0·35, which means that the model has significant skill and can be classified as reasonable. A regression coefficient of 0·66 is found for the observed and modelled mud content in the bed, which means that the model can reproduce the mud content reasonably well for most

locations. The model can clearly distinguish between a sand-dominated or mud-dominated area.

This model has proven to be a useful tool to predict morphological impacts in systems where both the sand and the mud fraction play a role in morphological changes.

6. Acknowledgements

The authors would like to thank the Dutch Ministry of Public Works for providing all the data used in this study.

REFERENCES

Borsje BW, De Vries MB, Hulscher SJMH *et al.* (2008) Modeling large-scale cohesive sediment transport affected by small-scale biological activity. *Estuarine, Coastal and Shelf Science* **78(3)**: 468–480.

Dam G (2008) *Buitendijks natuurherstel in de Westerschelde, verkenning naar mogelijke gebieden en maatregelen (Nature restoration in the Western Scheldt, research into possible areas and measures)*. Svašek Hydraulics, Rotterdam, the Netherlands, Report GD/08187/1480/C (in Dutch).

Dam G, Bliek AJ and Bruens AW (2005) Band width analysis morphological predictions Haringvliet Estuary. In *Proceedings of 4th IAHR Symposium of the River, Coastal and Estuarine Morphodynamics Conference, Urbana, USA* (Parker G and Garcia MH (eds)). Taylor & Francis, Leiden, the Netherlands, vol. 2, pp. 171–179.

Dam G, Bliek AJ, Labeur RJ *et al.* (2007) Long term process-based morphological model of the Western Scheldt estuary. In *Proceedings of 5th IAHR Symposium of the River, Coastal and Estuarine Morphodynamics Conference, Enschede, The Netherlands* (Dohmen-Janssen CM and Hulscher SJMH (eds)) Taylor & Francis, Leiden, the Netherlands, vol. 2, pp. 1077–1084.

Engelund F and Hansen E (1967) *A Monograph on Sediment Transport in Alluvial Channels*. Teknik Forlag, Copenhagen, Denmark.

Escaravage V, Sistermans WCH, Hummel H *et al.* (2007) *Studie naar de effecten van strekdammen op de bodemdieren gemeenschap van de slikken van Waarde in de periode 2002 tot 2007 (Study into effects of groynes on the bentic community on the mudflats of Waarde in the period 2002 to 2007)*. NIOO-CEME, Yerseke, the Netherlands (in Dutch).

Garcia-Navarro P and Saviron JM (1992) McCormack's method for the numerical simulation of one-dimensional discontinuous unsteady open channel flow. *Journal of Hydraulic Research* **30(1)**: 95–105.

Hibma A, De Vriend HJ and Stive MJF (2003) Numerical modelling of shoal formation in well-mixed elongated estuaries. *Estuarine, Coastal and Shelf Science* **57(5–6)**: 981–991.

Hibma A, Schuttelaars HM and De Vriend HJ (2004) Initial formation and long-term evolution of channel-shoal patterns. *Continental Shelf Research* **24(15)**: 1637–1650.

Koster Engineering (1997) *Stroom-en golfmetingen op slikken gelegen voor schorren in de Westerschelde (Current and wave measurements on mudflats in front of tidal marshes in the Western Scheldt)*. Koster Engineering, Heemstede, the Netherlands (in Dutch).

Krone RB (1962) *Flume Studies of the Transport of Sediment in Estuarial Shoaling Process.* Technical Report, Hydraulic Engineering Laboratory, University of California, Berkeley, CA, USA.

Marciano R, Wang ZB, Hibma A, de Vriend HB and Defina A (2005) Modeling of channel patterns in short tidal basins. *Journal of Geophysical Research: Earth Surface* **110(F1)**, http://dx.doi.org/10.1029/2003JF000092.

McClaren P (1994) *Sediment Transport in the Western Scheldt between Baarland and Rupelmonde*. GeoSea report, GeoSea Consulting, Cambridge, UK.

Mitchener H and Torfs H (1996) Erosion of mud/sand mixtures. *Coastal Engineering* **29(1–2)**: 1–25.

Paarlberg AJ, Knaapen MAF, De Vries MB *et al.* (2005) Biological influences on morphology and bed composition of an intertidal flat. *Estuarine, Coastal and Shelf Science* **64(4)**: 577–590.

Partheniades EA (1965) Erosion and deposition of cohesive soils. *Proceedings of the American Society of Civil Engineers – Journal of the Hydraulic Division* **91(1)**: 105–139.

Rijkswaterstaat (2012) *Waterbase*. See www.waterbase.nl (accessed 02/07/2012).

Roelvink JA (2006) Coastal morphodynamic evolution techniques. *Coastal Engineering* **53(2–3)**: 277–287.

Sieben J (2007) *Overzicht en synthese beschikbare data overlaatproeven (Overview and synthesis of available data of weir experiments)*. RIZA, Arnhem, the Netherlands, wrr memo 2007-003 (in Dutch).

Sistermans WCH, Hummel H, Bergmeijer MA *et al.* (2007) *Het macrobenthos van de slikken van Waarde in het voorjaar van 2002 (The macrobenthos of the mudflats of Waarde in the spring of 2002)*. NIOO-CEME, Yerseke, the Netherlands (in Dutch).

Sutherland J, Peet AH and Soulsby RL (2004) Evaluating the performance of morphological models. *Coastal Engineering* **51(8–9)**: 917–939.

Van der Spek AJF (1997) Tidal asymmetry and long-term evolution of Holocene tidal basins in The Netherlands: simulation of paleo-tides in the Schelde estuary. *Marine Geology* **141(1–4)**: 71–90.

Van der Wal D, Van Kessel T, Eleveld M *et al.* (2010) Spatial heterogeneity in estuarine mud dynamics. *Ocean Dynamics* **60(3)**: 519–533.

Van der Wegen M and Roelvink JA (2008) Long-term

morphodynamic evolution of a tidal embayment using a two-dimensional, process-based model. *Journal of Geophysical Research: Oceans* **113(C3)**, http://dx.doi.org/10.1029/2006JC003983.

Van der Wegen M and Roelvink JA (2012) Reproduction of estuarine bathymetry by means of a process-based model: Western Scheldt case study, the Netherlands. *Geomorphology* **179**: 152–167.

Van der Wegen M, Wang ZB, Savenije HHG and Roelvink JA (2008) Long-term morphodynamic evolution and energy dissipation in a coastal plain, tidal embayment. *Journal of Geophysical Research: Earth Surface* **11(F3)**, http://dx.doi.org/10.1029/2007JF000898.

Van Kessel T, Vanlede J and De Kok J (2010) Development of a mud transport model for the Scheldt estuary. *Continental Shelf Research* **31(10)**: 165–181.

Van Ledden M (2003) *Sand-mud Segregation in Estuaries and Tidal Basins*. PhD thesis, Delft University of Technology, the Netherlands.

Van Ledden M, van Kesteren WGM and Winterwerp JC (2004a) A conceptual framework for the erosion behaviour of sand-mud mixtures. *Continental Shelf Research* **24(1)**: 1–11.

Van Ledden M, Wang ZB, Winterwerp JC *et al*. (2004b) Sand-mud morphodynamics in a short tidal basin. *Ocean Dynamics* **54(3–4)**: 385–391.

Van Rijn LC (1993) *Principles of Sediment Transport in River, Estuaries and Coastal Seas*. Aqua Publications, Amsterdam, the Netherlands.

Van Rijn LC, Walstra DJR, Grasmeijer B *et al*. (2003) The predictability of cross-shore bed evolution of sandy beaches at the time scale of storms and seasons using process-based profile models. *Coastal Engineering* **47(3)**: 295–327.

Winterwerp JC and Van Kesteren WGM (2004) *Introduction to the Physics of Cohesive Sediment in the Marine Environment. Developments in Sedimentology* series, no. 56. Elsevier, Amsterdam, the Netherlands.